

ARTICLE OPEN

Deterministic preparation of highly non-classical macroscopic quantum states

Ludovico Latmiral¹ and Florian Mintert¹

We present a scheme to deterministically prepare non-classical quantum states of a massive mirror including highly non-Gaussian states exhibiting sizeable negativity of the Wigner function. This is achieved by exploiting the non-linear light–matter interaction in an optomechanical cavity by driving the system with optimally designed frequency patterns. Our scheme reveals to be resilient against mechanical and optical damping, as well as mechanical thermal noise and imperfections in the driving scheme. Our proposal thus opens a promising route for table-top experiments to explore and exploit macroscopic quantum phenomena.

npj Quantum Information (2018)4:44; doi:10.1038/s41534-018-0093-z

INTRODUCTION

Non-classicality of mechanical motion has recently been a topic of great interest both theoretically and experimentally as it represents a test ground to address many important questions ranging from quantum-to-classical transition and collapse models^{1–3} to the interface between quantum mechanics and gravity.^{4,5} While we have extensive literature that has focused on the quantumness of microscopic objects, it is a challenge to deterministically isolate genuine quantum features that can be accessed in experiments, and few experiments with coherent superpositions of quantum objects with large mass exist.^{6,7}

Massive mechanical oscillators have been intensively investigated in quantum optomechanics,^{8,9} and optomechanical cavities are regarded as an optimal framework to make clear comparisons between the predictions of classical theory and their quantum counterparts.^{10–15} Indeed, they were proven to exhibit a large degree of macroscopicity, μ , defined in terms of the robustness of a coherent superposition against decoherence.¹⁶ Optomechanical experiments have reached $\mu=19$ on a scale where the Mach–Zender interference of Cs¹⁷ and the Schrödinger gedanken experiment are attributed values of $\mu=10.6$ and $\mu\sim 55$, respectively.¹⁶

Thanks to their peculiar properties, these systems have been historically studied in the context of force sensing^{18,19} and for the preparation of non-classical states of the mechanical motion, such as squeezed states,^{20–24} single phonon excitations^{25–27} or even Schrödinger cat states.¹¹ Given the necessary interaction between optical and mechanical degrees of freedom, most control schemes result in the preparation of correlated states. The reduced state of the mechanical components is then strongly mixed, and a pure (or less strongly mixed) state can be obtained in terms of a measurement on the optical field.^{28,29} Since such a measurement has random outcomes, such a state preparation is intrinsically probabilistic. To the best of our knowledge, the only currently existing deterministic protocols rely on equilibration to a stationary state, being based on dissipative state preparation with the potential to prepare superpositions of two wave packets.^{30,31}

In this paper, we consider the deterministic preparation of highly non-classical, motional states via coherent control. Such a deterministic protocol, that permits to prepare non-stationary states, first of all helps to avoid the additional element of a measurement which is likely to be affected by limited detection efficiencies and dark counts. Since targeting states with increasing macroscopicity typically implies lower success rates of probabilistic protocols, this shall be helpful, in particular, for the experimental realisation of non-classical states of macroscopic character. Explicitly, we show how the non-linear light–matter interaction between an electromagnetic field and a movable mirror in an optomechanical cavity can be exploited to deterministically prepare on demand quantum states of the mirror such as squeezed states and non-Gaussian coherent superpositions exhibiting sizeable negativity of the Wigner function. Our control scheme proves to be resilient to several experimental imperfections, permitting maximally non-classical states to be achieved, which makes it ideal for accurate tests of fundamental physics, e.g. decoherence models, and of the technical potential of coherent superpositions of massive objects.

RESULTS

We consider an optomechanical cantilever modelled as harmonic oscillator of mass m , interacting with a light field through radiation pressure in the single mode approximation. This provides an accurate description for current experiments,^{9,21,26} though the techniques derived in the following also apply to optomechanical systems that are not based on cantilevers, or also more complex models including more degrees of freedom. The free evolution of the system is given by $\omega_c a^\dagger a + \omega_m b^\dagger b$, where ω_m (ω_c) is the mechanical (cavity resonance) frequency and b and b^\dagger (a and a^\dagger) are, respectively, the annihilation and creation operator of the mirror (cavity field). The interaction couples the intensity of the light field with the position of the mechanical element and is described by $H_{\text{int}} = -ga^\dagger a(b + b^\dagger)$,³² where $g = \omega_c \frac{\hbar}{L} = k\omega_m$ is the coupling constant, $L = \sqrt{\hbar/(2m\omega_m)}$ the oscillator length

¹QOLS, Blackett Laboratory, Imperial College London, London SW7 2AZ, UK
Correspondence: Ludovico Latmiral (ludovico.latmiral@hotmail.it)

Received: 13 January 2018 Revised: 20 August 2018 Accepted: 31 August 2018
Published online: 18 September 2018

scale, L_c the cavity length at equilibrium and $k = g/\omega_m$ the rescaled coupling.

Adding external driving $\xi(t)$ of the cavity, the complete Hamiltonian of the system reads $H = H_0 + H_{\text{int}}$ with $H_0 = \omega_c a^\dagger a + \omega_m b^\dagger b + i(\xi(t)a^\dagger - \xi^*(t)a)$. Generally the dynamics induces correlations between both subsystems. A correlated state, however, implies that a mixed quantum state needs to be attributed to each subsystem alone, or that the measurement on one of the subsystems results in the probabilistic preparation of the other.

The goal of the present paper lies in finding driving patterns $\xi(t)$ such that the cubic optomechanical interaction creates non-trivial states of the mirror without cavity–mirror correlations. In particular, the chosen driving profiles will also ensure that the cavity ends up in its initial state, which will significantly ease the readout subsequent to the state preparation. Indeed, most of the current state reconstruction techniques of mechanical motional states are achieved through homodyne tomography of a probe light field, i.e. the so called *back-action-evading interaction*.^{24,33,34} It is therefore an essential requirement that the cavity is in its well-defined initial state when the read out of the mechanics is performed.

In the limit of weak coupling $k \ll 1$, which is in agreement with state-of-the-art experiments operating at $k \lesssim 10^{-2}$,^{8,9} we can solve the dynamics in a perturbative expansion in powers of k . To this end, it is helpful to first find the time-evolution operator $U_0(t)$ induced by the non-interacting time-dependent Hamiltonian $H_0(t)$. Since $H_0(t)$ is harmonic, $U_0(t)$ is constructed exactly and it is subsequently used to extract the interaction Hamiltonian in the frame defined by the harmonic motion as $H_I(t) = U_0^\dagger(t) H_{\text{int}} U_0(t)$, which explicitly reads

$$H_I(t) = -g(n_c - (fa^\dagger + f^*a) + |f|^2)X_m(t), \quad (1)$$

with $X_m(t) = b^\dagger e^{i\omega_m t} + b e^{-i\omega_m t}$, $f = \int_0^t dt_1 \xi(t_1) e^{i\omega_c t_1}$ and $n_c = a^\dagger a$ the number operator of the cavity field.

Because of the cubic nature and the time-dependence, it is not possible to analytically solve the generator $V(t, t_0)$ induced by $H_I(t)$, but it can be obtained in the perturbative Magnus series³⁵ $V(t, t_0) = \exp\left(-i \sum_j \mathcal{M}_j(t, t_0)\right)$, where $\mathcal{M}_1(t, t_0) = \int_{t_0}^t dt_1 H_I(t_1)$, $\mathcal{M}_2(t, t_0) = -\frac{i}{2} \int_{t_0}^t dt_1 [H_I(t_1), \mathcal{M}_1(t_1, t_0)]$ and higher order terms \mathcal{M}_j satisfy the proportionality $\mathcal{M}_j(t, t_0) \sim k^j$.

Given the explicit form of $H_I(t)$ in Eq. (1), the lowest order term \mathcal{M}_1 is an interaction that induces correlations between cavity and mirror. The higher order expansions $\mathcal{M}_j (j > 1)$ will generally also contain both interaction and single-particle terms of mirror or cavity alone. Since the central goal of our work is deterministic state preparation, we will require that $\mathcal{M}_1(t)$ and undesired terms in $\mathcal{M}_j(t) (j > 1)$ vanish at the final instance in time $t = NT$, after N periods $T = 2\pi/\omega_m$ of the mechanical motion. We will design driving profiles $\xi(t)$ such that all interaction terms and all operators acting on the cavity vanish at $t = NT$, but such that the single-particle terms acting solely on the mirror induce highly non-classical states.

Since for a general time-dependent driving $\xi(t)$ it might be difficult to directly integrate the dynamics over N periods, it will prove useful to express the propagator $V(TN, 0)$ as

$$V(TN, 0) = \prod_{s=1}^N V(Ts, T(s-1)) = \prod_{s=1}^N \exp(-i\mathcal{M}^{(s)}),$$

where it is implied that terms are ordered with decreasing value of s in the product; the $\mathcal{M}^{(s)}$ are defined via the relation $\exp(-i\mathcal{M}^{(s)}) = V(Ts, T(s-1))$, and can be expanded in the Magnus series $\mathcal{M}^{(s)} = \sum_j \mathcal{M}_j^{(s)}$. Conversely, using Baker–Campbell–Hausdorff relation, we can rearrange all terms at the same order in the coupling, i.e. $\mathcal{M}_1(NT, 0) = \sum_{s=1}^N \mathcal{M}_1^{(s)}$

and similarly at higher orders. While there is no reason to expect light–matter correlations and cavity excitation terms to add up to zero at each order j in $\mathcal{M}_j(NT, 0)$, we propose time-dependent driving profiles $\xi_s(t)$ resulting in different interaction Hamiltonians $H_I^{(s)}(t)$ in each interval. With the specific choice $H_I^{(s)}(t) = W_s^\dagger H_I^{(1)}(t) W_s$ (with $W_1 = 1$), one obtains $V(TN, 0) = \prod_{s=1}^N W_s^\dagger V(T, 0) W_s = \prod_{s=1}^N \exp(-i\mathcal{M}^{(s)})$ with $\mathcal{M}^{(s)} = W_s^\dagger \mathcal{M}^{(1)} W_s$. Since all terms now depend on the W_s , which can be chosen freely, we will benefit from this freedom to ensure that any undesired term in \mathcal{M}_j vanishes or is modified as desired. As we will see in the following, there are clear physically motivated choices for the W_s that achieve the aim, and that translate into rather simple driving profiles.

Due to the large separation of the resonance frequencies of cavity and mirror ($\omega_c/\omega_m \sim O(10^7)$), it is essential to drive the former close to the sidebands with frequencies $\omega_c \pm \omega_m$ to enable the exchange of excitations between the two subsystems. We will hereafter find suitable profiles such that the mirror evolves into a strongly squeezed state as well as a state with pronounced non-Gaussian and non-classical features. Apart from an interest in its own, the discussion on strongly squeezed states shall help to exemplify the framework developed above, with simpler algebra than found in the preparation of non-classical states.

Mechanical squeezing is obtained via a bi-chromatic driving with detunings $\pm\omega_m$ with respect to the cavity resonance. The related driving profile $\xi_\omega(t) = E e^{-i\omega_c t} (e^{i\omega_m t} + e^{-i\omega_m t})$ with amplitude \mathcal{E} results in the lowest order contribution to the Magnus expansion after one period

$$\mathcal{M}_1^{(1)} = -2\pi k \eta X_c P_m, \quad (2)$$

with the dimensionless amplitude $\eta = \mathcal{E}/\omega_m$. This suggests the particularly simple choice $W_s = \exp(-in_c \varphi_s)$, that rotates cavity operators in phase space by an angle φ_s . The corresponding required driving profiles

$$\xi_s(t) = \mathcal{E} e^{i\varphi_s} e^{-i\omega_c t} (e^{i\omega_m t} + e^{-i\omega_m t}), \quad (3)$$

are obtained by reverse-engineering the derivation of the interaction Hamiltonian (see Eq. (1)) and are rather elementary to implement³⁶ (see Supplementary Materials). In fact, different driving periods differ from each other merely by the phase shift φ_s , such that Eqs. (2) and (3) result in

$$\sum_{s=1}^N \mathcal{M}_1^{(s)} = -2\pi k \eta \left(\sum_{s=1}^N X_c \cos \varphi_s + P_c \sin \varphi_s \right) P_m.$$

Hence, undesired interaction terms in \mathcal{M}_1 cancel for any choice satisfying $\sum_s \exp(i\varphi_s) = 0$.

The second-order contribution reads $\mathcal{M}_2(NT, 0) = \sum_{s=1}^N \mathcal{M}_2^{(s)} - \frac{i}{2} \sum_{s>l=1}^N [\mathcal{M}_1^{(s)}, \mathcal{M}_1^{(l)}]$ and contains correlations and single-particle excitation terms of the cavity that vanish upon the condition $\sum_s e^{i2\varphi_s} = 0$, which eventually motivates the selection $\varphi_s = 2\pi(s-1)/N$ (assuming $N > 2$).

The most important term in \mathcal{M}_2 for the creation of a mechanical squeezed state originates from the commutator $[\mathcal{M}_1^{(s)}, \mathcal{M}_1^{(l)}]$ and is proportional to $\propto (k\eta)^2 \sin(\varphi_s - \varphi_l) P_m^2$. With the choice $\varphi_s = 2\pi(s-1)/N$, the sum over all possible combinations $s > l = 1$ reads $\sum_{l<s} \sin(\varphi_s - \varphi_l) = \frac{N}{2} \cot\left(\frac{\pi}{N}\right)$, which scales $\sim N^2$ and thus becomes sizeable already after few periods of driving.

All-together, we have thus arrived at dynamics, such that no results of an interaction appear at the final instance in time and such that no excitations in the cavity have been created. Up to a global phase factor, which we will henceforth always neglect, the

full propagator reads $V_W(TN, 0) = V_c(N) \otimes V_m^{(2)}(N)$ with

$$V_c(N) = \exp(2\pi i N k^2 (n_c^2 + 7\eta^2 n_c)), \text{ and} \quad (4)$$

$$V_m^{(2)}(N) = \exp\left(2i(\pi k \eta)^2 N \cot\left(\frac{\pi}{N}\right) P_m^2\right).$$

$V_m^{(2)}(N)$ acts on the mirror only, and can be recast in the form

$$V_m^{(2)}(N) = e^{i\delta b^\dagger b} e^{\frac{1}{2}(\zeta^* b^2 - \zeta b^{\dagger 2})}, \quad (5)$$

corresponding to a vacuum squeezing operation with parameter

$$\zeta = i(2\pi k \eta)^2 N \cot\left(\frac{\pi}{N}\right) e^{i\delta},$$

and followed by a rotation with angle

$$\delta = \arctan\left((2\pi k \eta)^2 N \cot\left(\frac{\pi}{N}\right)\right).$$

The quadratic scaling with time (i.e. $|\zeta| \sim N^2$) allows substantial squeezing already after a few intervals. Besides, we should keep in mind that the perturbative regime requires reasonably short propagation times, i.e. small values of N , and the present analysis is valid in the limit $k \ll 1$, as the neglected third-order term scales as $\mathcal{M}_3 \sim k^3 \eta^2 N$. For a relatively weak interaction, $k = 1/400$, and sufficiently strong driving, $\eta = 10$, one achieves a squeezing of the position quadrature resulting, after $N = 11$ periods, in $\Delta P_m^2 = 1.57$ and $\Delta X_m^2 \simeq 0.16$ (see Fig. 1).

Let us now discuss the creation of non-Gaussian states, which requires to suppress not only interaction effects, but also Gaussian contributions to the dynamics, since these will tend to overshadow non-Gaussian features. We will therefore double the detuning as compared to Eq. (3), but employ qualitatively similar driving profiles

$$\xi_s(t) = \mathcal{E} e^{i\varphi_s} e^{-i\omega_c t} (e^{i2\omega_m t} + e^{-i2\omega_m t}), \quad (6)$$

with phase shifts φ_s whose form is to be determined.

Thanks to the chosen detuning, the first-order Magnus term \mathcal{M}_1 vanishes irrespectively of the choice for the φ_s . The second- and third-order contribution to the generator of the dynamics over N periods read $\mathcal{M}_2 = \sum_{s=1}^N \mathcal{M}_2^{(s)}$ and $\mathcal{M}_3 = \sum_{s=1}^N \mathcal{M}_3^{(s)}$ —in general, there would be contributions resulting from non-commutativity of $\mathcal{M}_{1/2}^{(s)}$ and $\mathcal{M}_1^{(l)}$, but in the present case those do not exist because $\mathcal{M}_1^{(s)}$ vanishes.

Even though $\mathcal{M}_2^{(s)}$ and $\mathcal{M}_3^{(s)}$ display a rather complicated form reflecting the complex dynamics induced by the non-linear Hamiltonian, it is still possible to ensure the desired goals of a product state with an empty cavity and a non-classical state of the mirror. This is achieved requiring every undesired element in

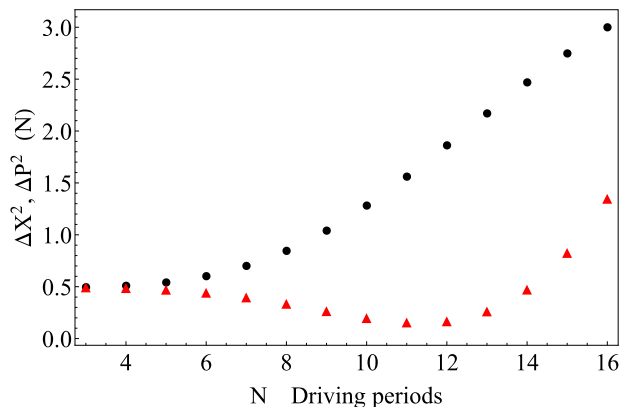


Fig. 1 Expected values for the quadratures of the mirror as a function of the total driving time expressed in terms of driving periods. Black circles represent ΔP^2 and red triangles ΔX^2 , which is squeezed by the evolution operator up to $\Delta X^2 = 0.16$. Experimental parameters are set as: $\eta = 10$, $k = 1/400$

$W_s^\dagger \mathcal{M}_j W_s$ ($j = 2, 3$) to be proportional to $\exp(\pm i\varphi_s)$ or $\exp(\pm i2\varphi_s)$, which would suggest to adopt the same set of phase shifts we proposed for the creation of squeezed states, i.e. $\varphi_s = 2\pi(s-1)/N$. Some care, however, is in order since preparing non-classical states relies on the dynamics induced by third-order terms in the coupling and thus requires a fairly stronger coupling regime. This makes an experimental realisation more challenging than the creation of squeezed states which is a second-order effect. On the other hand, the final propagator is enhanced by a factor η^2 , so that strong driving can compensate for the weak interaction. Yet, in the strong driving regime special care needs to be taken in the perturbative expansion: so far we were only concerned with powers of k , but for sufficiently large values of η , a high power of η can make a term relevant despite its high order in k . A quantitative analysis of the algebra and the perturbative expansion is provided in the Methods section; here we only outline that the propagator contains terms $\alpha k^2 \eta^2 n_c$ which create neither cavity excitations nor light-matter correlations, but which induce a back-action on the dynamics, rotating the field operators at each period and spoiling the effect of the previously engineered phase shifts. To counteract this effect that undermines the achievement of a separable state at the end of the N driving periods, we should modify the phase shift to

$$\varphi_s = \left(\frac{2\pi}{N} + \frac{4\pi}{3}(k\eta)^2\right)(s-1).$$

Making use of all the cancellations, we thus arrive at the desired separable propagator $V(TN, 0) = V_c(N) \otimes V_m^{(3)}(N)$ with

$$V_m^{(3)}(N) = \exp\left(-\frac{\pi}{3} i N k^3 \eta^2 Q_m\right), \text{ and} \quad (7)$$

$$V_c(N) = \exp(2\pi i k^2 (n_c^2 + \frac{2}{3} \eta^2 n_c) N),$$

defined in terms of the cubic operator

$$Q_m = \left(X_m + i \frac{P_m}{\sqrt{3}}\right)^3 + \left(X_m - i \frac{P_m}{\sqrt{3}}\right)^3 + \frac{3}{2} X_m. \quad (8)$$

In contrast to the well-characterised squeezed states discussed above, it is not clearly established what type of states are generated by Q_m . Hence, we construct $V_m^{(3)}(N)$ numerically in a truncated Hilbert space including up to 80×10^3 excitations. As prototype for discussion, we consider the state $|\Psi(20)\rangle = V_m^{(3)}(20)|0\rangle$ obtained after $N = 20$ periods of driving with the mirror initially in its ground state. As specific parameter values, we choose $\eta = 20$ and $k = 1/60$ consistently with the perturbative expansion and with up-to-date experimental achievements.^{8,9,37}

DISCUSSION

Since non-linear Hamiltonians tend to generate highly non-classical states, it is instructive to analyse the states that are accessible with the present control scheme in terms of commonly employed measures of non-classicality. A particularly intuitive approach can be derived in terms of the Wigner function $W(q, p) = \frac{1}{\pi} \int_{-\infty}^{\infty} \langle q + y | \rho | q - y \rangle e^{-2ipy} dy$, which is a quasi-probability distribution in phase space spanned by momentum and displacement variables p and q . Figure 2a depicts the Wigner function for the state $|\Psi(20)\rangle \langle \Psi(20)|$. Quantumness can be characterised by oscillations of $W(q, p)$, where high-amplitudes of short-wavelength oscillations including negative values imply deep quantum mechanical behaviour. As one can see, the Wigner function of $|\Psi(20)\rangle$ features short wavelength oscillations with large amplitudes. This is visible on a more quantitative level also in Fig. 2b, which shows the cut $W(q, 0)$ through the Wigner function.

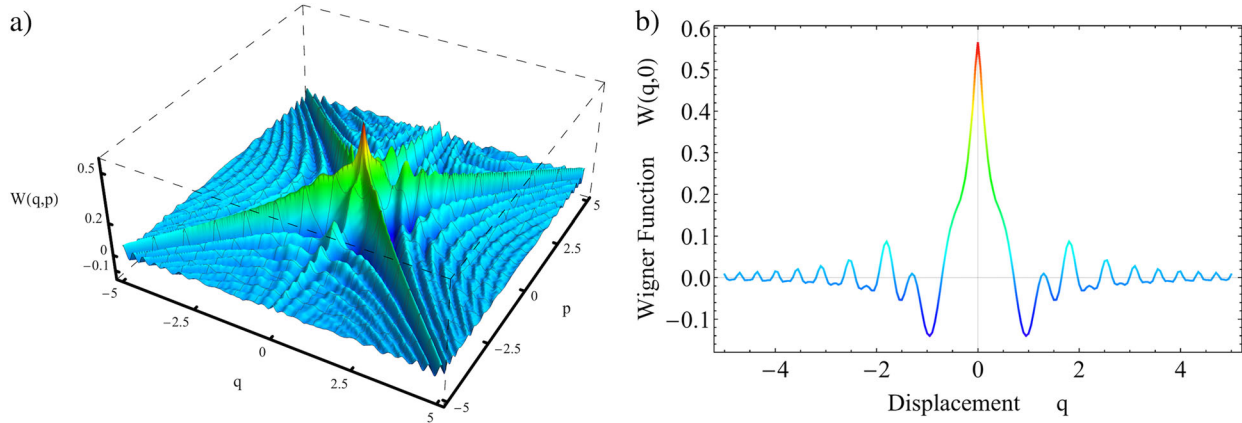


Fig. 2 **a** 3D Wigner function of the mirror after 20 driving periods and **b** its profile when it is cut by the plane $p=0$. The experimental parameters are set as $\eta=20$, $k=1/60$ and the resulting average population is $\langle b^\dagger b \rangle \simeq 20$

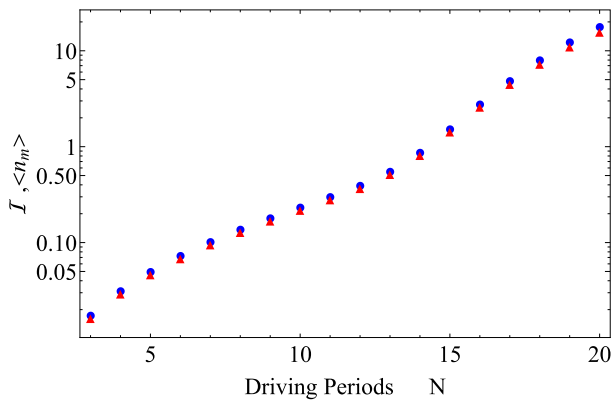


Fig. 3 Comparative plot of the non-classicality \mathcal{I} (red triangles) and the average number of mechanical excitations $\langle n_m \rangle$ (blue dots) as functions of the number of driving periods. The experimental parameters are set as $\eta=20$, $k=1/60$

In order to provide a quantitative estimate of the quantumness, we resort to the *measure of non-classicality*³⁸

$$\mathcal{I} = -\frac{\pi}{2} \int dp dq W(q,p) \left(\frac{\partial^2}{\partial q^2} + \frac{\partial^2}{\partial p^2} + 1 \right) W(q,p), \quad (9)$$

that quantifies fast oscillations of the Wigner function $W(q,p)$. This non-classicality \mathcal{I} lies in the interval $\mathcal{I} \in [0, \langle n \rangle]$, where $\langle n \rangle$ is the average number of excitations in the system. The minimal value $\mathcal{I}_{\min} = 0$ is obtained for classical states like Gaussian or thermal states, while purely quantum states, such as for example Fock and cat states, yield the maximum value of $\mathcal{I}_{\min} = \langle n \rangle$. We deem \mathcal{I} a more suitable figure of merit than macroscopicity, μ ,¹⁶ discussed in the introduction, since μ depends on system parameters like the particle mass, and thus, to a large extent characterises the experimental achievement of a challenging experiment with a massive object. \mathcal{I} , however, reflects solely on the conceptual added value of the present control scheme.

Figure 3 depicts \mathcal{I} as a function of the driving time expressed in units of mechanical periods (red triangles) together with the average population $\langle n \rangle$ (blue circles). Both quantities have an approximately exponential growth, so that highly excited, non-classical states can be prepared very quickly (we obtain $\langle n \rangle \simeq 18$ after $N=20$ periods). Moreover, quantumness nearly saturates the bound \mathcal{I}_{\max} imposed by the population, which witnesses the rapid evolution towards states of macroscopic character as well as their close-to-maximal non-classicality.

So far, we have discussed an idealised situation with unitary dynamics and no experimental imperfections. An extensive analysis of the resilience against experimental errors can be found in the Supplementary Materials. In particular, we analytically show how the driving profiles ensure robustness against optical and mechanical damping, as well as we provide evidence of the small detrimental effect of decoherence by numerically solving the full Lindbladian master equation. We also demonstrate that there is no fundamental need to require ground-state cooling preparation of the mirror, obtaining significant negative values of the Wigner function for an initial state with $\langle n_m^{\text{th}} \rangle = 1$, i.e. substantially above what is already achieved with sideband cooling. Importantly, also sizable deviations from the step-like phase shifts would not prevent the achievement of a highly non-classical state of the mirror and an empty cavity. Besides, we will argue that the proposed laser driving pattern can be accessed with state-of-the-art technology since phase shifts φ_s need to be implemented on long time scales that are of the order of $1/\omega_m$.

Thanks to the resilience to experimental imperfections, the massive mirror could be potentially used as continuous variable quantum memory, as it has already been proposed in ref.³⁹ or as probe for decoherence.^{3,31,40} The non-classicality \mathcal{I} of the mirror is an extremely sensitive indicator of any type of mechanical decoherence and is thus ideally suited to probe fundamental physics such as gravitationally induced effects on the mechanical motion or continuous spontaneous localisation.⁴¹

It should be highlighted that the utilised approach to find optimal driving patterns can be easily extended to higher orders in the Magnus expansion and correspondingly longer propagation times and/or larger coupling k . There is indeed no theoretical restriction to an adaptive fine tuning of the laser profiles to cancel undesired coupling terms in the evolution. This would give rise to more highly excited states and hence to measurable quantum effects also in case of higher initial thermal noise, pushing the initial cooling condition beyond the requirement $\langle n_m^{\text{th}} \rangle \lesssim 1$. The present control scheme is also not necessarily restricted to the mirror-cavity setup discussed here, but analogous techniques are suitable for a variety of systems that share similar non-linear hamiltonians such as atomic spin ensembles, trapped atoms or levitated nanoparticles.^{42–45}

METHODS

We provide full details on the reconstruction of the propagator induced by the Hamiltonian in Eq. (1) together with the driving profile in Eq. (5). Let us start by recalling the Magnus expansion for the propagator $V(T,0) = \exp(-i \sum_j \mathcal{M}_j^{(1)})$ over the first mechanical period. Thanks to the chosen

detuning, the first-order Magnus term \mathcal{M}_1 vanishes irrespectively of the choice for the φ_s .

The second- and third-order terms are

$$\begin{aligned}\mathcal{M}_2^{(1)} &= \pi k^2 (m_2^c + m_2^l - \frac{29}{60} \eta^4), \quad \text{with} \\ m_2^c &= -2n_c^2 + \frac{1}{3} \eta^2 (X_c^2 - 6n_c) \quad \text{and} \\ m_2^l &= \eta P_c (b^2 + b^{i^2});\end{aligned}\tag{10}$$

as well as $\mathcal{M}_3^{(1)} = \frac{\pi}{3} k^3 \eta (m_3^m + m_3^l)$, with

$$\begin{aligned}m_3^m &= [14i(a^l n_c - n_c a) - (\frac{36}{5} \eta^2 + 4) P_c] X_m \\ &+ [3X_c + 6i\eta(a^2 - a^{i^2})] P_m - \frac{3}{4} P_c Q_m,\end{aligned}\tag{11}$$

and $m_3^l = \eta Q_m$, with Q_m defined in Eq. (8)).

Exploiting the composition property, we write the identity $V(TN, 0) = \prod_{s=1}^N W_s^\dagger V(T, 0) W_s = \prod_{s=1}^N \exp(-iM^{(s)})$ with $\mathcal{M}^{(s)} = W_s^\dagger \mathcal{M}^{(1)} W_s$ and $W_s = \exp(-in_c \varphi_s)$. Choosing the same set of phase shifts as for the creation of mechanical squeezed states, i.e. $\varphi_s = 2\pi/N(s-1)$, one obtains

$$\begin{aligned}V(TN, 0) &= V_c(N) \otimes V_m^{(3)}(N), \quad \text{with} \\ V_c(N) &= \exp(2\pi i k^2 (n_c^2 + \frac{2}{3} \eta^2 n_c) N), \quad \text{and} \\ V_m^{(3)}(N) &= \exp(-\frac{\pi}{3} i N k^3 \eta^2 Q_m).\end{aligned}\tag{12}$$

Since the propagator for the mirror $V_m^{(3)}$ scales as $k^3 \eta^2$, the cubic dependence on k will make an experimental realisation more challenging than the creation of squeezed states which is a second-order effect. Given the quadratic dependence on η^2 , however, strong driving can compensate for the weak interaction. Yet, in the strong driving regime, special care needs to be taken in the perturbative expansion since a high power of η can make a term relevant despite its high order in k . In particular, $\mathcal{M}_2^{(1)}$ in Eq. (10) contains terms $\sim (k\eta)^2 n_c$, and terms $\sim (k\eta)^4$ resulting from the commutators $[\mathcal{M}_2^{(s)}, \mathcal{M}_2^{(l)}]$. This is not directly a severe issue for the state preparation, since such terms describe neither an interaction between cavity and mirror nor non-interacting dynamics of the mirror. They do induce, however, a perturbative rotation of the cavity field. As a result of that, the propagator at the end of the driving time does not factorise into individual propagators of mirror and cavity. It thus becomes necessary to change the driving profile accordingly to compensate for this effect.

In order to do so, it is instructive to rewrite the propagator over the first interval, neglecting terms of order $k^4 \eta^j$ with $j < 4$ and terms of order k^j with $j > 4$, as

$$\begin{aligned}V(T, 0) &\simeq e^{i\frac{\pi}{3} k^2 \eta^2 n_c} e^{-i\tilde{\mathcal{M}}^{(1)}}, \quad \text{with} \\ \tilde{\mathcal{M}}^{(1)} &= \pi k^2 (\tilde{m}_2^c + m_2^l) + \mathcal{M}_3^{(1)}, \quad \text{and} \\ \tilde{m}_2^c &= -2n_c^2 + \eta^2 (a^{i^2} + a^2 + 1)/3, \\ m_2^l &= \eta P_c (b^2 + b^{i^2}),\end{aligned}\tag{13}$$

where the term $\exp(i\frac{4}{3} \pi k^2 \eta^2 n_c)$ in the expression for $V(T, 0)$ —and similarly for $V(sT, (s-1)T)$ —is the undesired rotation. The propagator over N periods can be written as

$$V(TN, 0) = W_{N+1}^\dagger \left(\prod_{s=1}^N W_{s+1} W_s^\dagger V(T, 0) \right) W_1,$$

and we should choose the W_s such that the prefactors $W_{s+1} W_s^\dagger$ cancel the term $e^{i\frac{4}{3} \pi k^2 \eta^2 n_c}$ in Eq. (13). This is achieved with the set of phases

$$\varphi_s = \left(\frac{2\pi}{N} + \frac{4\pi}{3} (k\eta)^2 \right) (s-1),$$

which counterbalances exactly the phase shift $\Delta = \frac{4\pi}{3} k^2 \eta^2$ that the cavity experiences through the driving over each period as described in Eq. (13). With this, the propagator reads

$$V(TN, 0) = \prod_{s=1}^N \exp\left(e^{\frac{2\pi i}{N}(s-1)n_c} M^{(1)} e^{-\frac{2\pi i}{N}(s-1)n_c} \right),\tag{14}$$

and the basic principles discussed in main text for the cancellation of all the interaction and cavity excitation terms apply. Quite importantly, however, the terms $\sim (k\eta)^2 n_c$ no longer appear, and the only remaining contribution scaling as $\sim (k\eta)^2$ in m_2^c in Eq. (13) is the polynomial $a^{i^2} + a^2 + 1$. Operators a^{i^2} and a^2 cancel out exactly in the summation over the N periods, thanks to the specific set of phase shifts, and the '+ 1' brings an irrelevant global phase. The terms $\sim (k\eta)^4$ arising from the

commutators $[\mathcal{M}_2^{(s)}, \mathcal{M}_2^{(l)}]$ (which are of the form $(a^2, a^{i^2}) = 4n_c + 2$) contribute either to the global phase or to a global final rotation in V_c . Lastly, we will see that the only term $\sim (k\eta)^4$ in $M_4^{(1)}$ depends on P_c and averages out in the summation over the N periods. The explicit final form of Eq. (13) coincides with Eq. (12) and the one given in the main text.

DATA AVAILABILITY

This is a theoretical paper and there is no experimental data available beyond the numerical simulation data described in the paper.

ACKNOWLEDGEMENTS

We are grateful for fruitful discussions with Michael Vanner and Benjamin Dive. This work was supported by the European Research Council within the project ODYCQUENT.

AUTHOR CONTRIBUTIONS

All authors made substantial contributions and were involved in drafting and writing the article.

ADDITIONAL INFORMATION

Supplementary information accompanies the paper on the *npj Quantum Information* website (<https://doi.org/10.1038/s41534-018-0093-z>).

Competing interests: The authors declare no competing interests.

Publisher's note: Springer Nature remains neutral with regard to jurisdictional claims in published maps and institutional affiliations.

REFERENCES

- Marshall, W., Simon, C., Penrose, R. & Bouwmeester, D. Towards quantum superpositions of a mirror. *Phys. Rev. Lett.* **91**, 130401 (2003).
- Romero-Isart, O. Quantum superposition of massive objects and collapse models. *Phys. Rev. A* **84**, 052121 (2011).
- Bahrami, M., Paternostro, M., Bassi, A. & Ulbricht, H. Proposal for a non-interferometric test of collapse models in optomechanical systems. *Phys. Rev. Lett.* **112**, 210404 (2014).
- Pikovski, I., Vanner, M. R., Aspelmeyer, M., Kim, M. S. & Brukner, Č. Probing planck-scale physics with quantum optics. *Nat. Phys.* **8**, 393–397 (2012).
- Bawaj, M. et al. Probing deformed commutators with macroscopic harmonic oscillators. *Nat. Commun.* **6**, 7503 (2015).
- Hackermüller, L. et al. Wave nature of biomolecules and fluorofullerenes. *Phys. Rev. Lett.* **91**, 090408 (2003).
- Hackermüller, L., Hornberger, K., Brezger, B., Zeilinger, A. & Arndt, M. Decoherence of matter waves by thermal emission of radiation. *Nature* **427**, 711 (2004).
- Kippenberg, T. J. & Vahala, K. J. Cavity optomechanics: back-action at the mesoscale. *Science* **321**, 1172 (2008).
- Aspelmeyer, M., Kippenberg, T. J. & Marquardt, F. Cavity optomechanics. *Rev. Mod. Phys.* **86**, 1391 (2014).
- Mancini, S., Man'ko, V. I. & Tombesi, P. Ponderomotive control of quantum macroscopic coherence. *Phys. Rev. A* **55**, 3042 (1997).
- Bose, S., Jacobs, K. & Knight, P. L. Preparation of nonclassical states in cavities with a moving mirror. *Phys. Rev. A* **56**, 4175 (1997).
- Bose, S., Jacobs, K. & Knight, P. L. Scheme to probe the decoherence of a macroscopic object. *Phys. Rev. A* **59**, 3204 (1999).
- Yang, H., Miao, H., Lee, D. S., Helou, B. & Chen, Y. Macroscopic quantum mechanics in classical spacetime. *Phys. Rev. Lett.* **110**, 170401 (2013).
- Latmiral, L., Armata, F., Genoni, M. G., Pikovski, I. & Kim, M. S. Probing anharmonicity of a quantum oscillator in an optomechanical cavity. *Phys. Rev. A* **93**, 052306 (2016).
- Armata, F. et al. Quantum and classical phases in optomechanics. *Phys. Rev. A* **93**, 063862 (2016).
- Nimmrichter, S. & Hornberger, K. Macroscopicity of mechanical quantum superposition states. *Phys. Rev. Lett.* **110**, 160403 (2013).
- Isenhowe, L., Williams, W., Dally, A. & Saffman, M. Atom trapping in an interferometrically generated bottle beam trap. *Opt. Lett.* **34**, 1159 (2009).
- Caves, C. M., Thorne, K. S., Drever, R. W. P., Sandberg, V. D. & Zimmermann, M. On the measurement of a weak classical force coupled to a quantum-mechanical oscillator. i. issues of principle. *Rev. Mod. Phys.* **52**, 341 (1980).

19. Braginsky, V., Khalili, F., & Thorne, K. (1992). Quantum Measurement. Cambridge: Cambridge University Press. <https://doi.org/10.1017/CBO9780511622748>.
20. Kronwald, A., Marquardt, F. & Clerk, A. A. Arbitrarily large steady-state bosonic squeezing via dissipation/arbitrarily large steady-state bosonic squeezing via dissipation. *Phys. Rev. A* **88**, 063833 (2013).
21. Wollman, E. E. et al. Quantum squeezing of motion in a mechanical resonator. *Science* **349**, 952 (2015).
22. Pirkkalainen, J.-M., Damskäg, E., Brandt, M., Massel, F. & Sillanpää, M. Squeezing of quantum noise of motion in a micromechanical resonator. *Phys. Rev. Lett.* **115**, 243601 (2015).
23. Lecocq, F., Clark, J. B., Simmonds, R. W., Aumentado, J. & Teufel, J. D. Quantum nondemolition measurement of a nonclassical state of a massive object. *Phys. Rev. X* **5**, 041037 (2015).
24. Lei, C. U. et al. Quantum nondemolition measurement of a quantum squeezed state beyond the 3 db limit. *Phys. Rev. Lett.* **117**, 100801 (2016).
25. Rips, S., Kiffner, M., Wilson-Rae, I. & Hartmann, M. J. Steady-state negative wigner functions of nonlinear nanomechanical oscillators. *New J. Phys.* **14**, 023042 (2012).
26. Qian, J., Clerk, A. A., Hammerer, K. & Marquardt, F. Quantum signatures of the optomechanical instability. *Phys. Rev. Lett.* **109**, 253601 (2012).
27. Børkje, K. Scheme for steady-state preparation of a harmonic oscillator in the first excited state. *Phys. Rev. A* **90**, 023806 (2014).
28. Abdi, M., Pernpeintner, M., Gross, R., Huebl, H. & Hartmann, M. J. Quantum state engineering with circuit electromechanical three-body interactions. *Phys. Rev. Lett.* **114**, 173602 (2015).
29. Liao, J.-Q. & Tian, L. Macroscopic quantum superposition in cavity optomechanics. *Phys. Rev. Lett.* **116**, 163602 (2016).
30. Asjad, M. & Vitali, D. Reservoir engineering of a mechanical resonator: generating a macroscopic superposition state and monitoring its decoherence. *J. Phys. B* **47**, 045502 (2014).
31. Abdi, M., Degenfeld-Schonburg, P., Sameti, M., Navarrete-Benlloch, C. & Hartmann, M. J. Dissipative optomechanical preparation of macroscopic quantum superposition states. *Phys. Rev. Lett.* **116**, 233604 (2016).
32. Law, C. K. Interaction between a moving mirror and radiation pressure: a hamiltonian formulation. *Phys. Rev. A* **51**, 2537 (1995).
33. Zhang, J., Peng, K. & Braunstein, S. L. Quantum-state transfer from light to macroscopic oscillators. *Phys. Rev. A* **68**, 013808 (2003).
34. Clark, J. B., Lecocq, F., Simmonds, R. W., Aumentado, J. & Teufel, J. D. Sideband cooling beyond the quantum backaction limit with squeezed light. *Nature* **541**, 191 (2017).
35. Blanes, S., Casas, F., Otero, J. A. & Ros, J. The magnus expansion and some of its applications. *Phys. Rep.* **470**, 151 (2009).
36. Thom, J., Wilpers, G., Riis, E. & Sinclair, A. G. Accurate and agile digital control of optical phase, amplitude and frequency for coherent atomic manipulation of atomic systems. *Opt. Express* **21**, 18712 (2013).
37. Teufel, J. D. et al. Sideband cooling of micromechanical motion to the quantum ground state. *Nature* **475**, 359 (2011).
38. Lee, C.-W. & Jeong, H. Quantification of macroscopic quantum superpositions within phase space. *Phys. Rev. Lett.* **106**, 220401 (2011).
39. Chan, J. et al. Laser cooling of a nanomechanical oscillator into its quantum ground state. *Nature* **478**, 89 (2011).
40. Romero-Isart, O. et al. Large quantum superpositions and interference of massive nanometer-sized objects. *Phys. Rev. Lett.* **107**, 020405 (2011).
41. Ghirardi, G. C., Pearle, P. & Rimini, A. Markov processes in hilbert space and continuous spontaneous localization of systems of identical particles. *Phys. Rev. A* **42**, 78 (1990).
42. Myatt, C. J., King, B. E., Turchette, Q. A. & Sackett, C. A. Decoherence of quantum superpositions through coupling to engineered reservoirs. *Nature* **493**, 269 (2000).
43. Julsgaard, B., Kozhekin, A. & Polzik, E. S. Experimental long-lived entanglement of two macroscopic objects. *Nature* **413**, 400 (2001).
44. Scala, M., Kim, M. S., Morley, G. W., Barker, P. F. & Bose, S. Matter-wave interferometry of a levitated thermal nano-oscillator induced and probed by a spin. *Phys. Rev. Lett.* **111**, 180403 (2013).
45. Hammerer, K. et al. Strong coupling of a mechanical oscillator and a single atom. *Phys. Rev. Lett.* **103**, 063005 (2009).



Open Access This article is licensed under a Creative Commons Attribution 4.0 International License, which permits use, sharing, adaptation, distribution and reproduction in any medium or format, as long as you give appropriate credit to the original author(s) and the source, provide a link to the Creative Commons license, and indicate if changes were made. The images or other third party material in this article are included in the article's Creative Commons license, unless indicated otherwise in a credit line to the material. If material is not included in the article's Creative Commons license and your intended use is not permitted by statutory regulation or exceeds the permitted use, you will need to obtain permission directly from the copyright holder. To view a copy of this license, visit <http://creativecommons.org/licenses/by/4.0/>.

© The Author(s) 2018